First design of a post-collision line CLIC at 3 TeV

T. Ekelöf, P. Eliasson, A. Ferrari, V. Ziemann*

June 20, 2006

Abstract

As part of the Post-Collision Diagnostic Lattice task of the ILPS work-package of EuroTeV, we discuss a design of the beam line between the interaction point and the beam dump for CLIC with a center-of-mass energy of 3 TeV. The design is driven by the requirement to transport the beam and all secondaries, such as beamstrahlung photons and coherent pairs, to the beam dump with minimal losses. Moreover, we discuss the integration of novel diagnostic methods into the CLIC post-collision beam line, based on the detection of coherent pairs and monitoring the beam profile of the primary beam.

*All authors at Uppsala University, Sweden

1 Introduction

The design of a post-collision line at CLIC [1] is driven by the need to minimize beam losses, in order to avoid irradiation of the detector by back-scattered secondaries. This task is made very difficult by the fact that the energy spread of the outgoing beams almost reaches 100 %. There is an abundance of low-energy particles that are likely be over-focused in quadrupoles, as shown in Ref. [2], where the 20 mrad post-collision line of ILC [3] was exposed to the CLIC outgoing beams. The losses could be reduced by down-scaling all magnet excitations. However, the optics of the extraction line was destroyed at the nominal energy, which prevents from measuring the outgoing beams. We use this indication to investigate minimal solutions without any focusing element, retaining only a simple chicane to prevent a direct line-of-sight from the dump into the detector and to separate the primary beam from the beamstrahlung photons and the e^+e^- coherent pairs, thus allowing their use for diagnostics purposes.

A further constraint comes from the thin window that separates the water-based beam dump from the accelerator vacuum. This window must withstand the 20 MW beam power, not only when the beams are in collision and thus widened by the strong beam-beam interactions, but also in the case of non-colliding beams which, due to their very small emittances, are much smaller on the window, thus leading to a much higher local energy deposition. With no quadrupole that can affect the beam size, the distance from the interaction point to the dump window is constrained by the requirement that the colliding beams fit within the window and that the distance is large enough to avoid an excessive local heating of the window in the case of non-colliding beams. Under normal conditions, the vertical beam size on the dump window is smaller than the horizontal one. The chicane will thus be vertical in order to facilitate the separation between the primary beam and the beamstrahlung photons. Also, a horizontal chicane would bend the opposite-charge particles of the coherent pairs back onto the incoming beam line.

2 Post-collision line layout

The layout of the CLIC post-collision line will be mostly determined by the properties of the incoming beam and by the beam-beam effects at the interaction point (IP) which are calculated with GUINEA-PIG [4] and are collected in Table 1. The rms angular divergence of the non-colliding beams are 5 and 10 μrad and, for the colliding beams, these numbers increase to 66 and 24 μrad, respectively. Also, the beam-beam effects may increase significantly when there is a small vertical offset in angle and/or position between the colliding beams. This mostly affects the vertical angular divergences of the disrupted beam and the beamstrahlung photons, which may both reach 80 μrad [2]. Assuming a dump window diameter of 20 cm and a post-collision line length of 150 m, we get at least a 7-sigma clearing of the window.

Parameters	Value	Unit
Beam energy	1.5	TeV
Particles per bunch	2.56×10^9	
Bunches in train	220	
Length of pulse train	100	ns
Repetition rate	150	Hz
Average current	13.5	μA
Beam power	20.3	MW
H/V beta function at IP	16, 0.07	mm
H/V emittance at IP	225, 7	fm-rad
H/V beam size at IP	60, 0.7	nm
H/V divergence at IP	3.75, 10	μrad
Post-IP x'/y' (outgoing beam)	33, 26	μrad
Post-IP x'/y' (beamstrahlung)	66, 24	μrad

Table 1: Beam parameters at the CLIC interaction point.

In order to accommodate a detector of unknown but large size, we assume that the chicane starts 24 m after the IP. Its first part consists of three dipole magnets with a length of 4 m and a field of 1 T each. The total bending angle is 2.4 mrad and will allow the separation of the primary beam from both the beamstrahlung photons and the opposite-charge particles of the coherent pairs. The first downward bend of the chicane is immediately followed by a bend in the opposite direction, which also consists of three dipole magnets with a length of 4 m and a field of 1 T each. As a result, taking into account a spacing of 1 m between two consecutive magnets, the separation between the disrupted beam and the beamstrahlung photons at the dump is 3.6 cm, see Figure 2. These plots were obtained after a particle tracking with DIMAD [5], however no aperture limitations were included.

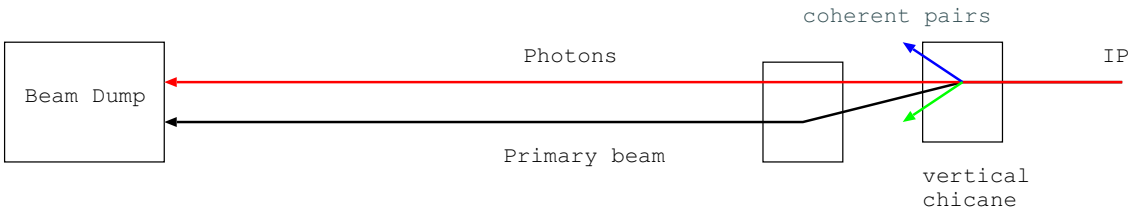

Figure 1: Schematic layout of the CLIC post-collision line, where each bend is provided by three dipole magnets.

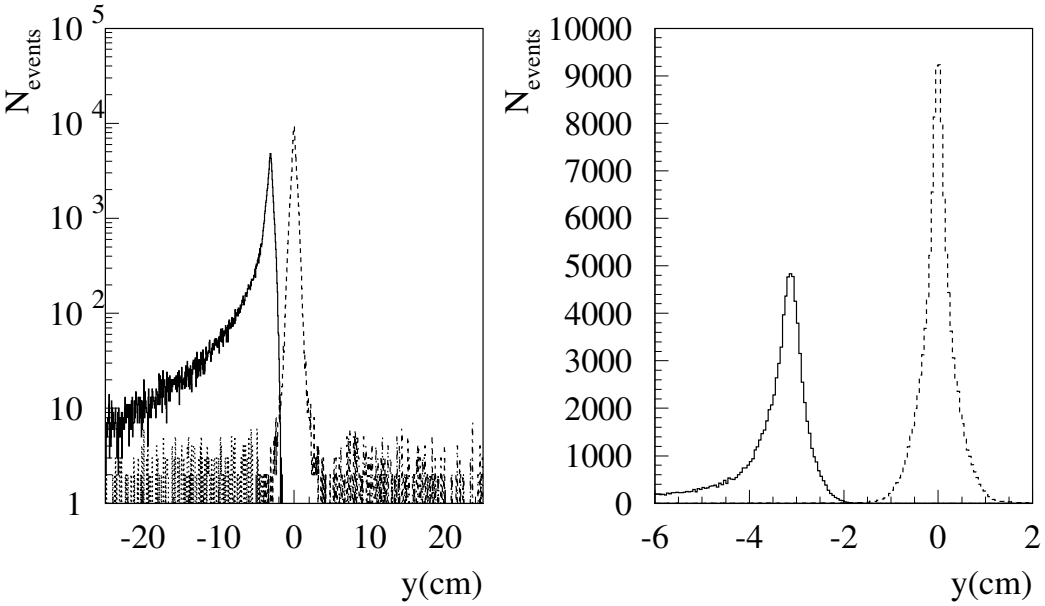

Figure 2: Vertical beam distribution 100 m downstream of the post-collision magnetic chicane, for the disrupted beam (full line), the beamstrahlung photons (dashed line) and the e^+e^- coherent pairs (dotted and dot-dashed lines).

3 Beam losses in the chicane

Various constraints must be taken into account for the design of the CLIC post-collision extraction magnets. In particular, a compromise must be found between the amount of lost particles and the size of the vacuum pipe in the gap (and thus of the magnet itself), keeping in mind the proximity of the incoming beam line. Detailed particle trackings, with aperture limitations and misalignments, were performed with DIMAD for this purpose. In order to keep both the power losses and the magnet dimensions at a reasonable level, we found that collimators should be installed between two consecutive dipoles. This allows to bring down the power losses in all magnets below 1 kW, at the cost of depositing up to 7-8 kW on the collimators, especially in the central part of the chicane. Most of the beam losses in the post-collision chicane come from the low-energy particles, which are found both in the tail of the disrupted beam and in the coherent pairs, see Figure 3. Here, the vertical line pattern is due to the structure of the DIMAD output where losses are assigned to each element of the beam line, instead of being continuously distributed.

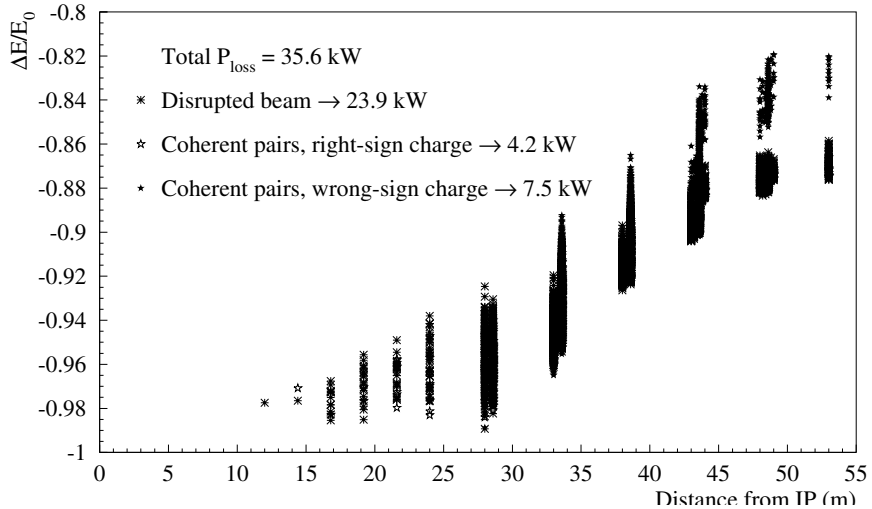

Figure 3: Relative energy spread of the lost particles as a function of the position of loss in the post-collision chicane.

Future studies should focus on the impact of these beam losses on the design of the collimators and the magnets, but also on the background at the interaction point. The beam pipe at the exit of the chicane has a height of 50 cm, in order to accept the disrupted beam and the coherent pairs, while we expect it to be at least twice smaller at the dump. One should therefore extract the particles of the coherent pairs with the wrong-sign charge and consider either additional collimators or some soft focusing in order to reduce the size of the disrupted beam and the particle of the coherent pairs with the right-sign charge.

4 Design of the dump window

The dump window at the end of the post-collision line, which we assume to be made of copper, is very similar to other exit windows that are penetrated by high-energy electron beams. A thorough analysis of the requirements for such windows was done in Ref. [6], which we follow.

We already mentioned that the window should have a radius $R = 10\,\mathrm{cm}$. If we assume a pressure difference $\Delta p = 1\,\mathrm{bar}$ (0.1 MPa) and a window thickness $d = 3\,\mathrm{mm}$, the stress on the dump window is $\sigma = 0.49\Delta p R^2/d^2 = 55\,\mathrm{MPa}$, well below the stress limit of 200 MPa for copper, thus providing some safety margin. Since the thickness of the window is significantly smaller than the radiation length of copper, no shower develops and only ionization losses with a magnitude $(dE/dx)/\rho = 2.35\,\mathrm{MeV/cm^2g}$ will occur in the window [7].

The most severe thermal stress on the dump window is caused by the non-colliding beam, which has horizontal and vertical rms sizes of 1.5 mm and 0.56 mm. The instantaneous temperature rise due to the impact of a bunch train with $N_{train} = 220 \times 2.56 \cdot 10^9$ particles will generate a temperature rise $\hat{T}$ of

$$\hat{T} = \frac{1}{\rho}\left(\frac{dE}{dx}\right)\frac{N_{train}e}{2\pi\sigma_x\sigma_y C_v} = 10.5\,\mathrm{K} \tag{1}$$

where the heat capacity of copper C_v is $0.385\,\mathrm{J/gK}$.

The value of about 10 K is very moderate compared with ILC, mostly due to a lower number of particles per bunch train. The cyclic stress due to the temperature increase is rather modest: $\sigma_c = \alpha E\hat{T}/2 = 9.5\,\mathrm{MPa}$, where $E = 110\,\mathrm{GPa}$ is Young's modulus and $\alpha = 16.5 \times 10^{-6}/\mathrm{K}$ is the thermal expansion coefficient.

A bunch train impinges on the dump window at a rate of 150 Hz and heats the window at the center, from where the heat diffuses to the edge, that we assume to be held at a fixed temperature of 37 C. In order to simplify the calculations, we assume a circular symmetry and numerically solve the corresponding heat conduction equation with a periodic excitation:

$$\frac{\partial T}{\partial t} = \frac{D}{r}\frac{\partial}{\partial r}r\frac{\partial T}{\partial r} + \sum_n \hat{T}\delta(t - n\Delta t), \tag{2}$$

where the thermal diffusion constant is $D = 1.1\,\mathrm{cm^2/s}$ for copper.

The evolution of the temperature at the center of the dump window and the radial distribution are shown in Figure 4. All involved temperatures remain very moderate and will not cause any problem.

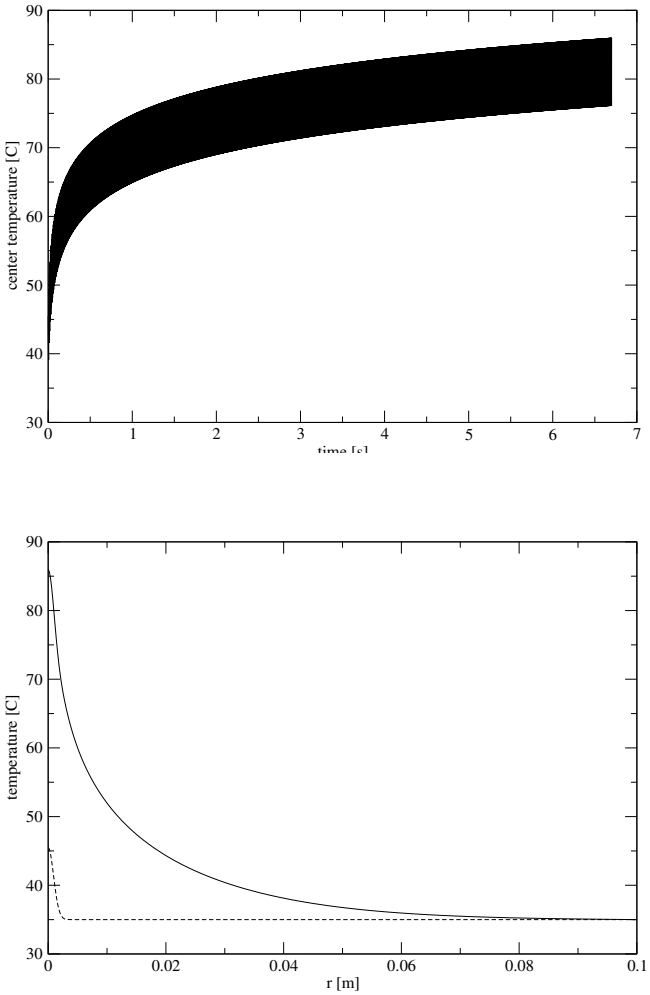

Figure 4: Temperature evolution at the center of the dump window (top) and radial temperature distribution at $t = 0\,\mathrm{s}$ and $t = 6.7\,\mathrm{s}$ (bottom).

Using two windows, spaced by 2 mm, and filling the thin region between them with a laminar flowing sheet of water will provide extra cooling of the windows, as well as some extra protection in case of window failure. Furthermore, if the water flows horizontally, monitoring its vertical temperature distribution, e.g. with the interferometric thermometer proposed in Ref. [8], will provide a signal related to the vertical energy deposition and thereby information on the angular divergence at the interaction point.

5 Conclusion and outlooks

We presented a first design of the CLIC post-collision beam line, based on a vertical chicane with six magnets and collimators to keep the power losses in the dipoles below 1 kW. Also, we performed an analysis of the dump window at the end of the post-collision line. Both the stress and the temperature rise remain well below the limits. Moreover, using an interferometric thermometer, we propose to measure the transverse distributions of the disrupted beam and the beamstrahlung photons at the dump. Their transport from the exit of the chicane still has to be simulated. Also, we plan to study the extraction of the particles of the coherent pairs with the wrong-sign charge and their use for diagnostics purpose.

Acknowledgements

This work is supported by the Commission of the European Communities under the 6^{th} Framework Programme "Structuring the European Research Area", contract number RIDS-011899.

The authors wish to thank D. Reistad and T. Zickler for fruitful discussions on the post-collision magnet design.

References

[1] CLIC Study Team, *A 3 TeV e^+e^- Linear Collider based on CLIC Technology*, CERN 2000-008, 2000.

[2] A. Ferrari, *Power losses of a nominal CLIC beam in the ILC 20 mrad extraction line*, EUROTeV-Report-2006-019.

[3] R. Arnold, et.al., *Design of ILC extraction line for 20 mrad crossing angle*, Proceedings of PAC 2005, Knoxville, USA.

[4] D. Schulte, *Study of electromagnetic and hadronic background in the Interaction Region of TESLA*, PhD-thesis, TESLA-97-08.

[5] http://www.slac.stanford.edu/accel/ilc/codes/dimad

[6] M. Seidel, *An Exit Window for the TESLA Test Facility*, DESY-TESLA 95-18, August 1995.

[7] S. Seltzer, M. Berger, *Improved Procedure for Calculating the Collision Stopping Power of Elements and Compounds for Electrons and Positrons*, Int. J. Appl. Radiat. Isot. 35 (1984) 665.

[8] V. Ziemann, *Ideas for an Interferometric Thermometer*, accepted for publication in Nucl. Inst. and Meth. A, 2006.